SCIENCE CHINA
Physics, Mechanics & Astronomy

• Article •

September 2014 Vol. 57 No. 9: 1644–1648
doi: 10.1007/s11433-014-5405-5

Electrical and thermal transport properties of CdO ceramics

LÜ Qing, WANG ShuFang*, LI LongJiang, WANG JiangLong*, DAI ShouYu,
YU Wei & FU GuangSheng

Hebei Key Lab of Optic-Electronic Information and Materials, College of Physics Science and Technology, Hebei University,
Baoding 071002, China

Received August 27, 2013; accepted October 12, 2013; published online March 25, 2014

High temperature electrical and thermal transport properties, that is, electrical conductivity, Seebeck coefficient and thermal conductivity, of CdO ceramics have been investigated. Because of the good electrical properties and low thermal conductivity, the dimensionless figure-of-merit *ZT* of the CdO ceramics reaches 0.34 at 1023 K. This value is comparable to the best reported *ZT* for the n-type oxide ceramic thermoelectric materials and remains as potential to be further improved by porosity controlling or nanostructuring.

CdO ceramics, electrical transport properties, thermal conductivity, solid state reaction

PACS number(s): 72.80.Ga, 72.20.Pa, 81.20.Ev

Citation: Lü Q, Wang S F, Li L J, et al. Electrical and thermal transport properties of CdO ceramics. Sci China-Phys Mech Astron, 2014, 57: 1644–1648, doi: 10.1007/s11433-014-5405-5

1 Introduction

Thermoelectric (TE) systems are direct energy conversion devices for converting thermal flux to electric power, and the reverse, transforming electric power directly to pumping heat from a cold source to a hot heat sink. The critical factor to realize an efficient TE systems lies in finding good materials with high TE performance, low-cost as well as good chemical and thermal stability in air. The performance of a TE material is evaluated by the dimensionless figure of merit $ZT=(S^2\sigma/\kappa)T$, where S, σ, κ and T are the Seebeck coefficient, electrical conductivity, thermal conductivity and absolute temperatures, respectively. Therefore, good TE materials should possess large power factor $S^2\sigma$ and low thermal conductivity κ which contains the phonon thermal conductivity κ_{ph} and the carrier thermal conductivity κ_e.

According to the thermoelectric transport theories, the ZT at optimal doping is a function of a parameter $\mu(m^*/m_0)^{3/2}/\kappa_{ph}$ and is found to increase monotonically with this parameter, where μ is the carrier mobility, m^* and m_0 is the carrier effective mass and the free electron mass, respectively [1,2]. Thus the state-of-the-art TE materials are primarily intermetallic compounds and alloys with high mobility, heavy constituting elements as well as low Debye temperature which can lead to a low phonon thermal conductivity κ_{ph} [3]. However, these materials often suffer from poor antioxidation in air, low abundance and high cost of the constituting elements. Oxide TE materials can overcome these problems and therefore have attracted increasing attention to the TE community. In the past decade, layered cobalt oxides, $SrTiO_3$ or $CaMnO_3$-based perovskite-type oxides, transpararent conductive oxides (TCOs) and tetragonal tungsten bronze ferroelectrics (Sr, Ba)$Nb_2O_{6-\delta}$ have been extensively studied as promising oxide TE materials for high temperature applications [4–16]. Compared with p-type oxide TE materials, most n-type oxide TE materials have inferior performance because of high thermal conduc-

---

*Corresponding author (WANG ShuFang, email: swang2008@hotmail.com; WANG JiangLong, email: jlwang@hbu.edu.cn)

tivities. For example, the maximal *ZT* value so far obtained in $SrTiO_3$- and ZnO-based ceramics has been 0.35 and 0.47 (~1000 K), respectively [6,13]. Therefore, searching for new n-type oxides with good TE performance is crucial for the development of oxide TE devices.

Cadmium oxide (CdO) is a heavily doped semiconductor that has high conductivity because of a large number of donor impurities which are thought to be either Cd interstitials or oxygen vacancies [17]. CdO is usually used as a transparent conductive material for photoelectric devices and there have been many reports on the optical and electrical properties. Compared with ZnO, CdO has the similar carrier effective mass m^*, but higher carrier mobility, heavier constituting elements and lower Debye temperature [18]. These attractive features indicate CdO might show a good TE performance. However, there are few reports on the TE properties of CdO, particularly on high temperature TE properties. Recently, we reported on the TE performace of porous Er-doped CdO ceramics fabricated through resolving metal Cd (99.8%) in nitric acid and a reasonable *ZT* of 0.2 was obtained in the 0.5% doped sample at 723 K [19]. Herein we investigated the high temperature TE properties of dense CdO ceramics sintered by commercial CdO powders (Alfa Aesar) and gave more focus to understanding the electrical and thermal transport mechanisms of the samples. We attain a high *ZT* of about 0.34 at 1023 K in the dense CdO ceramics. This value is comparable to the best *ZT* reported so far for the n-type oxide ceramic TE materials and appears to have potential to be further improved by porosity controlling or nanostructuring.

2 Experimental

The CdO ceramics were synthesized by the conventional solid state reaction technique. The commercial CdO powder (99.95%, Alfa Aesar) was used as the starting material. After grinding, they were compacted in pellets at 10 MPa and then sintered in air at 800°C for 20 h in a furnace. Table 1 lists the density and the main transport parameters of a CdO ceramic sample measured at room temperature. The density was determined by the Archimedes method. The carrier concentration n and carrier mobility μ were measured by using Van Der Pauw method. The electrical resistivity ρ and Seebeck coefficient S were simultaneously measured by the standard dc four-probe technique with a LSR-3 measurement system (Linseis, Germany) in a low-pressure helium atmosphere. The thermal conductivity κ was calculated from the density d, specific heat capacity C_p, and thermal diffusivity D values according to the equation $\kappa=DC_pd$, here C_p was measured using a differential scanning calorimeter (Netzsch DSC200F3) and D was measured using the laser flash technique on LFA457 system (Netzsch, Germany). The structure of the sample was examined by powder X-ray diffraction (XRD) analysis with Cu Kα radiation (D8, Bruke). All the peaks in the XRD pattern, shown in Figure 1, can be indexed to CdO with space group $Fm\bar{3}m$ (PDF#780653). The inset of Figure 1 presents the scanning electron microscopy (SEM) image from the fractured cross-section of the CdO sample. It consists of large and dense-packed grains with size between 2 μm and 6 μm.

3 Results and discussion

The ρ-T curve shown in Figure 2(a) reveals that the resistivity increases with increasing temperature, reaches the maximumal value at around 923 K and then decreases. This ρ-T behavior has been observed in many other heavily doped semiconductors and can be explained in the following manner. In extrinsic temperature regime with lower temperatures, the number of thermally excited charge carriers is very small and the electrical conductivity is primarily determined by the extrinsic carriers. As the temperature increases, the thermally excited intrinsic carriers across the energy gap can not be ignored and thus commence to contribute to the resistivity, within intrinsic temperature regime with higher temperatures, then the number of thermally excited intrinsic carriers will exceed that of the extrinsic carriers and subsequently leads to the intrinsic conduction becoming predominate [20]. Moreover, the resistivity in the

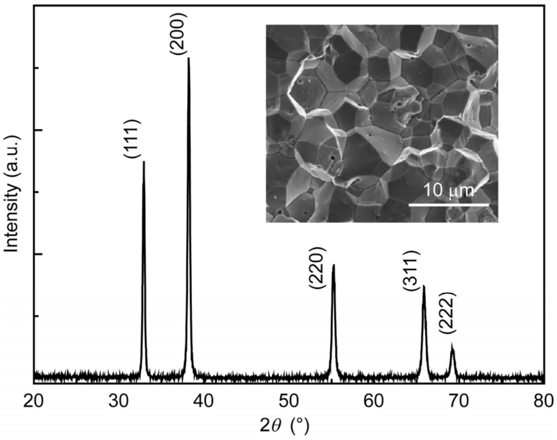

Figure 1 XRD θ-2θ scanning pattern of the CdO ceramic sample. The inset is the cross-sectional SEM micrograph of the sample.

Table 1 Room temperature Density (d), carrier concentration (n), Hall mobility (μ), resistivity (ρ), Seebeck coefficient (S), thermal conductivity (κ) for the present CdO ceramic sample

CdO	d (g/cm^3)	n (10^{19} cm^{-3})	μ (cm^2/(V s))	ρ (μΩ m)	S (μV/K)	κ (W/(m K))
	8.0	2.5	148.0	16.9	−76.0	8.1

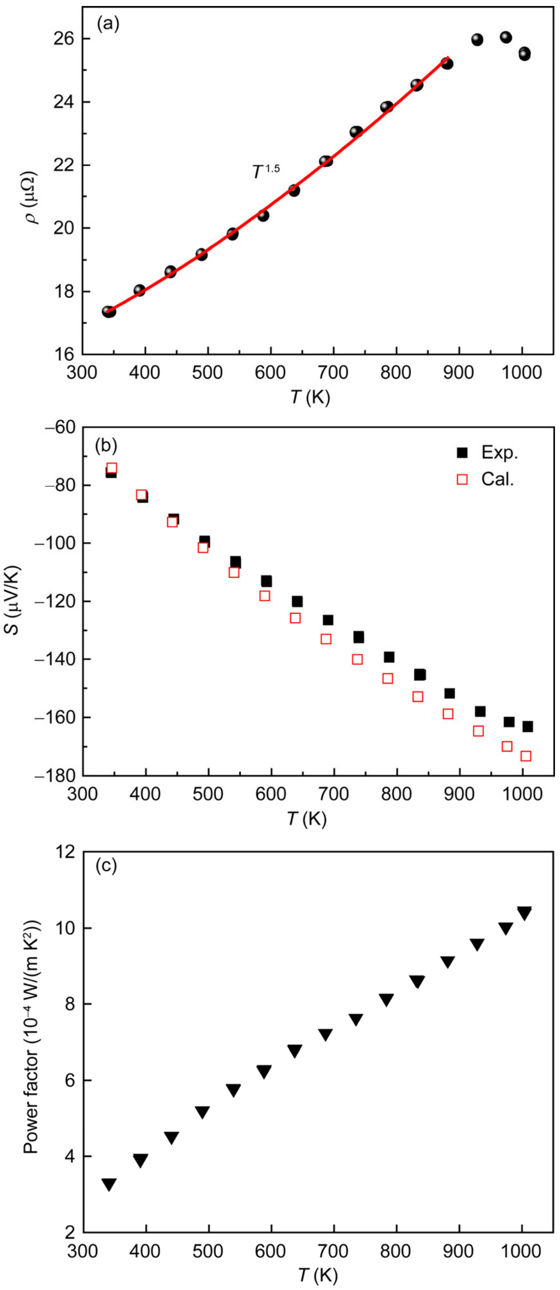

Figure 2 (Color online) Temperature dependence of (a) resistivity ρ and (b) Seebeck coefficient S and (c) power factor S^2/ρ of the CdO ceramic sample. The solid line of (a) reveals that the resistivity ρ increases proportionally to $T^{1.5}$ below 923 K and the open square in (b) represents the theoretical calculation for acoustic phonon scattering of electrons $\gamma=-1/2$.

extrinsic regime (T<923 K), where the charge carrier density is nearly independent of temperature, which exhibits a strong temperature dependence in the form of $\rho \propto T^{1.5}$, suggesting the acoustic phonon scattering is the dominant carrier scattering mechanism for the present CdO sample in this temperature range [21].

Figure 2(b) presents the corresponding S-T curve of the same CdO sample. The sign of S was negative, indicating an n-type conducting. The absolute value of the Seebeck coefficient, $|S|$, increases with increasing temperature in the extrinsic region and then decreases because of the contribution of the thermally excited carrier. We have theoretically calculated S according to the the following equations [22]:

$$S=-\frac{k_{\mathrm{B}}}{e}\left(\frac{\left(r+\frac{5}{2}\right)F_{r+\frac{3}{2}}(\eta)}{\left(r+\frac{3}{2}\right)F_{r+\frac{1}{2}}(\eta)}-\eta\right), \tag{1}$$

$$F_r(\eta)=\int_0^{\infty}\frac{\varepsilon^r}{1+e^{\varepsilon-\eta}}\mathrm{d}\varepsilon, \tag{2}$$

$$n=4\pi\frac{(2m^{*}\kappa_{\mathrm{B}}T)^{3/2}}{h^3}F_{1/2}(\eta), \tag{3}$$

where k_{B} is the Boltzmann constant, r is the scattering parameter of relaxation time and r=−1/2 for the acoustic phonons scattering obtained by fitting the electrical resistivity data, η is reduced Fermi energy, F_r is the Fermi integral, m^* is the carrier effective mass, and h is the Plank constant, respectively. Our experimental measured Seebeck coefficient S_{exp} is in good agreement with the calculated Seebeck coefficient S_{cal} in the extrinsic region and the departure of the S_{exp} from the S_{cal} is because of the contribution of the thermally excited carrier. Moreover, the carrier effective mass of CdO estimated from eqs. (1)–(3) is about $0.27m_0$ (m_0 is the free electron mass), which is coincident well with the value recently obtained in epitaxial CdO thin films [23].

At room temperature, the CdO sample has a thermal conductivity κ of about 8 W/(m K) (Figure 3(a)), which is more than 7-fold lower than that of ZnO ceramics and is comparable to that of nanostructured ZnO bulks [14,15]. The low thermal conductivity κ in CdO is suggested to be related to the heavy constituting elements as well as low Debye temperature, which will result in a small phonon thermal conductivity κ_{ph} and therefore a small total thermal conductivity κ. At the highest measured temperature of 1023 K, the κ of the sample is about 3.3 W/(m K), which is comparable to the Al-Ga dually doped ZnO [13]. The inverse thermal conductivity $1/\kappa$ as a function of the temperature plotted in the inset of Figure 3(a) shows an excellent linearity in the extrinsic region (T<923 K), suggesting that the thermal transport is dominated by the Umklapp process between the phonons in this temperature range [12]. This suggestion is further confirmed by predominated proportion of the phonon thermal conductivity shown in Figure 3(b), which is calculated from the overall κ by subtracting the electron thermal conductivity κ_{e} and κ_{e} is estimated by the Wiedemann-Franz law $\kappa_{\mathrm{e}}=L_0T\sigma$ with the Lorentz number $L_0=2.45\times10^{-8}$ V^2 K^{-2}.

The temperature variations of the calculated ZT value of the CdO sample is shown in Figure 4. At the highest measured

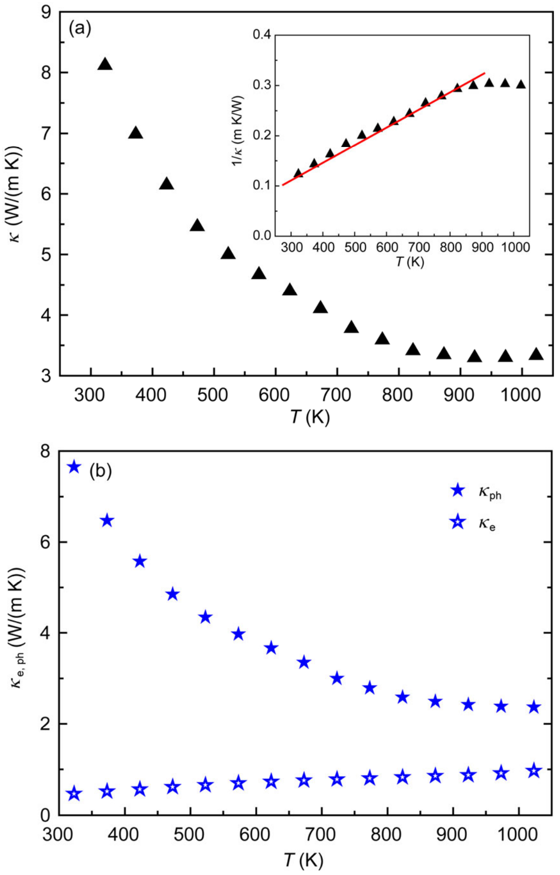

Figure 3 (Color online) Temperature dependence of (a) thermal conductivity κ and (b) phonon thermal conductivity κ_{ph} and electron thermal conductivity κ_e of the CdO ceramic sample. The inset of (a) shows inverse thermal conductivity $1/\kappa$ as a function of the temperature below 923 K and the solid line is guide for eye.

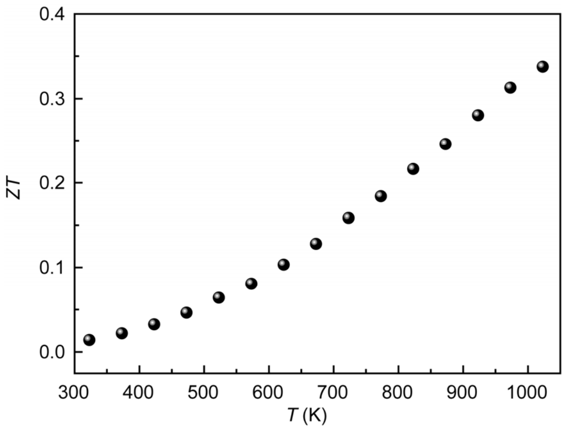

Figure 4 Temperature dependence of *ZT* for the CdO ceramic sample.

temperature of 1023 K, the *ZT* is about 0.34. To test the reproducibility of our results, we have measured several CdO samples sintered with same conditions and an almost consistent peak *ZT* value was obtained at 1023 K. This *ZT* value is comparable to that reported for the best n-type oxide ceramic TE materials and still has potential to be further improved by porosity controlling or nanostructuring. For example, we are experimenting with the porous CdO ceramics and a *ZT* of 0.45 has been achieved at 1023 K in the best sample.

4 Conclusion

We have investigated the high temperature electrical and thermal transport properties of dense CdO ceramics. A high *ZT* of 0.34 can be achieved in such dense samples at 1023 K because of the good electrical properties and low thermal conductivity. Further improvement in *ZT* is possible by nanostrctureing or porosity controlling. Our research demonstrates that CdO show a promising TE performance besides the good electrical and optical properties.

This work was supported by the Natural Science Foundation for Distinguished Young Scholars of Hebei Province (Grant No. A2013201249) and the National Natural Science Foundation of China (Grant No. 51372064).

1 Rowe D M, Bhandari C M. Modern Thermoelectrics. Virginia: Reston Publishing Company, 1983
2 Tritt T M. Recent Trends in Thermoelectric Materials Research I: Semiconductor and Semimetals. San Diego: Academic Press, 2001
3 Roufosse M, Klemens P G. Thermal conductivity of complex dielectric crystals. Phy Rev B, 1973, 7: 5379–5386
4 Koumoto K, Terasaki I, Funahashi R. Complex oxide materials for potential thermoelectric applications. MRS Bull, 2006, 31: 206–210
5 Nong N V, Pryds N, Linderoth S, et al. Enhancement of the thermoelectric performance of p-type layered oxide $Ca_3Co_4O_9$ through heavy doping and metallic nanoinclusions. Adv Mater, 2011, 23: 2484–2490
6 Ohta H, Kim S, Komune Y, et al. Giant thermoelectric Seebeck coefficient of a two-dimensional electron gas in $SrTiO_3$. Nat Mater, 2007, 6: 129–134
7 Ohta S, Ohta H, Kaumoto K, et al. Grain size dependence of thermoelectric performance of Nb-Doped $SrTiO_3$ polycrystals. J Ceram Soc Jpn, 2006, 114: 102–105
8 Wang H C, Wang C L, Su W B, et al. Doping effect of La and Dy on the thermoelectric properties of $SrTiO_3$. J Am Ceram Soc, 2011, 94: 838
9 Bocher L, Aguirre M H, Logvinovich D, et al. $CaMn_{1-x}Nb_xO_3$ ($x \leqslant 0.08$) perovskite-type phases as promising new high-temperature n-Type thermoelectric materials. Inorg Chem, 2008, 47: 8077–8085
10 Bérardan D, Guilmeau E, Maignan A, et al. In_2O_3: Ge, a promising n-type thermoelectric oxide composite. Solid State Commun, 2008, 146: 97–101
11 Jung K H, Lee K H, Seo W S, et al. An enhancement of a thermoelectric power factor in a Ga-doped ZnO system: A chemical compression by enlarged Ga solubility. Appl Phys Lett, 2012, 100: 253902
12 Ohtaki M, Tsubota T, Eguchi K, et al. High-temperature thermoelectric properties of $(Zn_{1-x}Al_x)O$. J Appl Phys, 1996, 79: 1816–1718
13 Ohtaki M, Araki K, Yamamoto K. High thermoelectric performance of dually doped ZnO ceramics. J Electron Mater, 2009, 38: 1234–1238
14 Tsubota T, Ohtaki M, Eguchi K, et al. Thermoelectric properties of Al-doped ZnO as a promising oxide material for high-temperature

thermoelectric conversion. J Mater Chem, 1997, 7: 85–90

15 Jood P, Mehta R J, Zhang Y L, et al. Al-doped zinc oxide nanocomposites with enhanced thermoelectric properties. Nano Lett, 2011, 11: 4337–4342

16 Lee S, Bock J A, Trolier-McKinstry S, et al. Ferroelectric-thermoelectricity and Mott transition of ferroelectric oxides with high electronic conductivity. J Eur Ceram Soc, 2012, 32: 3971–3988

17 Koffyberg F P. Electron concentration and mobility in semimetallic CdO. Canadian J Phys, 1971, 49: 435–440

18 Madelung O, Rössler U, Schulz M. II-VI and I-VII Compounds: Semimagnetic Compounds. New York: Springer-Verlag, 1999

19 Wang S F, Liu F Q, Lü Q, et al. The effect of Er^{3+} doping on the structure and thermoelectric properties of CdO ceramics. J Euro Ceram Soc, 2013, 33: 1763–1768

20 Kuznetsova L A, Kuznetsov V L, Rowe D M. Thermoelectric properties and crystal structure of ternary compounds in the Ge(Sn, Pb)Te-Bi_2Te_3 systems. J Phys Chem Solids, 2000, 61: 1269–1274

21 Ohta S, Nomura T, Ohta H, et al. High-temperature carrier transport and thermoelectric properties of heavily La- or Nb-doped $SrTiO_3$ single crystals. J Appl Phys, 2005, 97: 034106

22 Vining C B. A model for the high-temperature transport properties of heavily doped n-type silicon-germanium alloys. J Appl Phys, 1991, 69: 331–341

23 Vasheghani-Farahani S K, Muñoz-Sanjosé V, Zúñiga-Pérez J, et al. Temperature dependence of the direct bandgap and transport properties of CdO. Appl Phys Lett, 2013, 102: 022102